JOURNAL OF APPLIED ELECTROCHEMISTRY 26 (1996) 1027–1035

Impedance and transient study of aluminium barrier-type oxide films

S. GUDIĆ, J. RADOŠEVIĆ, M. KLIŠKIĆ

Faculty of Technology, Laboratory of Electrochemistry, Split, Croatia

Received 31 October 1995; revised 2 February 1996

The effect of the passivation potential on the properties of the barrier films formed on high purity aluminium has been examined. The current–time responses were recorded, the charge used during formation of the barrier film was determined, and the steady-state currents were discussed. Impedance measurements provided an insight into the characteristic sizes of barrier films. Equivalent circuits which illustrate the examined aluminium/oxide film/electrolyte systems were proposed and individual circuit elements were defined. The resistance and thickness of the barrier film were shown to increase linearly with increase in the passivation potential, while increase in solution pH caused a marked decrease in the total system impedance. The paper also defines current efficiency in the formation of the barrier film. The value of ~20% indicates that the formation of barrier films on aluminium is a process that takes place with considerable current losses. The mechanism of barrier film growth has been examined within the framework of two models suggested by different authors. Both agreements with and differences from the theories proposed have been indicated.

1. Introduction

Great attention has been paid to the problem of oxide film formation as oxide films make it possible for many important industrial metals and alloys to be used in environments where it would not have been otherwise possible. Various models have been proposed during the last fifty years in an attempt to explain growth kinetics. One of the earliest models is that of Cabrera and Mott [1], in which the rate-limiting step (r.l.s.) for film growth is the emission of metal cations from the metal into the film, and metal cation diffusion is responsible for film growth. In the 'place-exchange' mechanism [2, 3] the r.l.s. is the emission of the anion from the environment into the film, and the activation energy of the r.l.s. increases linearly with thickness. The field-limited mechanism [4, 5] states that the anodic oxidation is limited by the field in the film. MacDougall *et al.* [6–8] have proposed a model which considers the defect character of the oxide film where film perfection increases logarithmically with time. Macdonald *et al.* [9–11] proposed a point defect model which is based on the migration of point defects in the electrostatic field within the film.

When aluminium is anodically oxidized in neutral solutions of borates, tartrates or certain organic acids, 'compact' barrier type oxide films are formed. The properties and growth kinetics of anodically formed aluminium oxide films have been investigated mostly on relatively thick barrier type oxide films with thickness of the order of 100 nm [12–14], using standard potentiostatic and galvanostatic measurement techniques as well as electrochemical impedance spectroscopy (EIS). The properties and growth kinetics of thin oxide films, thinner than 10 nm, on aluminium have been less extensively investigated. The most important contributions were those by Bessone *et al.* [15, 16] who used EIS to examine the relatively thin anodically formed barrier type films in ammonium tartrate solutions.

This work examines the growth kinetics and the properties of relatively thin barrier-type films on high purity aluminium in neutral and alkaline solutions of borate buffer. This was done by following the decay of the anodic current upon step polarization into the passive region, and by measuring the impedance of the Al/oxide film/electrolyte system. The results were correlated with the two point defect models.

2. Experimental details

The electrodes were of high purity aluminium (99.999%), obtained by courtesy of Alcan International. The aluminium sample was cut into cubes and made into electrodes by inserting insulated copper wires and protecting all sides but one with epoxy resin. Before each measurement the surface pretreatment was performed by mechanical polishing of the electrode surface up to a mirror finish followed by alkali attack by immersing the electrode for 4 min in 0.1 M NaOH at 40 °C. The electrode was then rinsed in doubly-distilled water. The exposed geometric area was 0.57 cm^2. A conventional three-compartment Pyrex cell was used with a large platinum sheet (9 cm^2) and a saturated calomel electrode (SCE), connected to the cell by a Luggin capillary, serving as the counter and the reference

0021-891X

electrodes, respectively. The measurements were performed at a constant temperature of 25 ± 0.1 °C in borate buffer solutions with different values of pH (6.8, 7.8, 8.4 and 9.25) with stirring, under nitrogen. The solutions were prepared from analytical grade chemicals and doubly-distilled water.

Electrochemical measurements were performed using a PAR model 273 potentiostat (EG&G) driven by a computer (PC 386SX). Transient measurements were performed to follow the rapid decrease of current after an anodic potential step. After stepping the potential, the electrode was kept for 1 h at a chosen potential in the passive potential region investigated (from −0.2 to 2.0 V). When performing impedance measurements, beside the equipment described, a lock-in amplifier PAR model 5210 (EG&G) was used. The EIS spectra were obtained under potentiostatic conditions after holding the electrode at the chosen potential for 1 h. The impedance data were found to be independent of the perturbation signal amplitude, ΔE, in the range $5\,\text{mV} \leqslant \Delta E \leqslant 15\,\text{mV}$. The experimental value chosen was $\Delta E = 10\,\text{mV}$. The frequency range studied was $30\,\text{mHz} \leqslant f \leqslant 50\,\text{kHz}$.

3. Results and discussion

3.1. *Polarization measurements*

Figure 1 shows the polarization plots for aluminium in borate buffer solutions for two different pH values, obtained by applying a linear potential perturbation at a sweep rate, $v = 5\,\text{mV s}^{-1}$. No active–passive transition was noticed in the anodic polarization of aluminium in any of the solutions examined. There was a small and practically constant current between −0.5 and 2.0 V, marking the passive region. An analysis of the polarization plots indicates that the passivation currents for aluminium increase with solution pH.

3.2. *Transient measurements*

Figure 2 shows a typical current-time response recorded during formation of the oxide film on

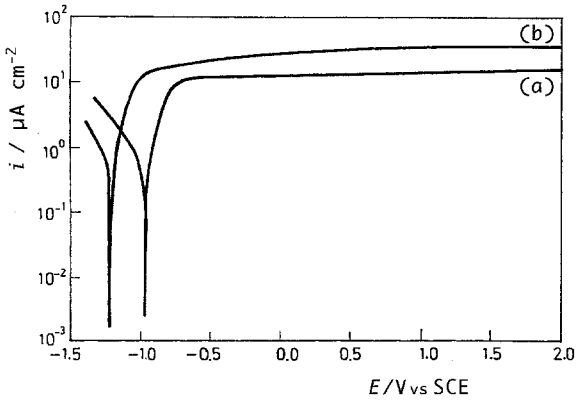

Fig. 1. Polarization plots for aluminium in borate buffer solutions of different pH values: (a) 6.8; (b) 9.25.

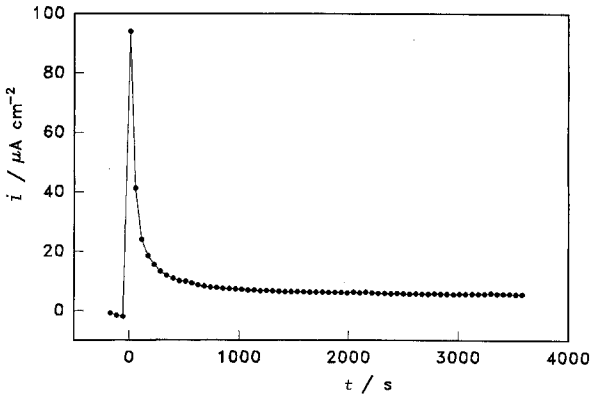

Fig. 2. Current–time responses obtained during aluminium passivation at a potential of 0.6 V in the borate buffer solution pH 7.8.

aluminium in borate buffer solution (pH 7.8) at 0.6 V. A characteristic decrease of current with anodizing time was observed in all cases. A decrease in the anodic current with time reflects oxide film formation. As the current established during the oxide film formation process is a measure of the protective capability of the oxide, its decrease with time is due to the increases thickness of the oxide film and/or the ordering of the oxide film structure. Eventually, a steady-state current, i_{ss}, is reached. By integrating the surface under the current–time responses, using the following equation:

$$Q_A = \int_0^t (i - i_{ss})\,dt \qquad (1)$$

the quantity of charge, Q_A, used during film formation was determined. The data in Table 1 indicate that for passivation in a solution of pH 7.8 the calculated Q_A increases from 3.94 to 18.68 mC cm^{-2} when the passivation potential increases from −0.2 to

Table 1. Results of the analysis of current–time responses for aluminium as a function of applied potential and solution pH

pH	*E vs SCE* /V	*k* /mA cm^{-2}	*m*	Q_A /mC cm^{-2}	*d* /nm
6.8	0.0	0.3	0.73	4.50	2.47
	0.6	0.3	0.64	8.32	4.58
	1.2	0.4	0.63	13.01	7.16
7.8	−0.2	0.3	0.73	3.94	2.17
	0.0	0.3	0.73	4.28	2.35
	0.2	0.4	0.71	5.29	2.91
	0.4	0.4	0.67	7.18	3.95
	0.6	0.4	0.64	8.81	4.85
	0.8	0.4	0.63	10.72	5.90
	1.0	0.4	0.61	11.82	6.50
	1.2	0.5	0.63	13.65	7.51
	1.4	0.6	0.61	15.60	8.58
	1.6	0.6	0.61	16.92	9.31
	1.8	0.7	0.60	17.53	9.64
	2.0	0.8	0.59	18.68	10.27
8.4	0.0	0.4	0.73	5.14	2.83
	0.6	0.4	0.64	9.79	5.38
	1.2	0.6	0.63	14.17	7.79
9.25	0.0	3.3	–	5.27	2.90
	0.6	4.3	–	12.47	6.86
	1.2	5.6	–	20.65	11.36

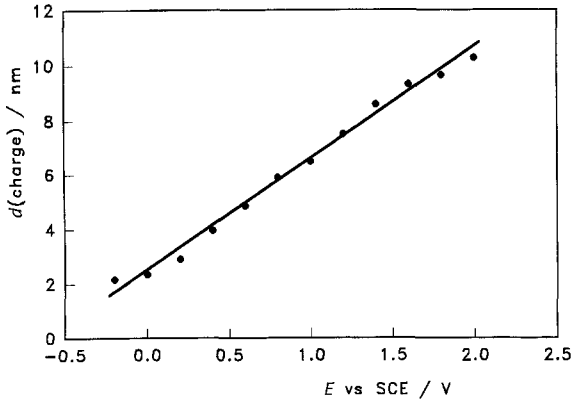

Fig. 3. Barrier film thickness (determined from the quantity of charge) relative to passivation potential for the borate buffer solution pH 7.8.

2.0 V. The measured anodic charge after 1 h of anodization was transformed to film thickness, using

$$\Delta d = \frac{MQ_A}{\rho z F} \qquad (2)$$

where ρ is the oxide density ($3.2\,g\,cm^{-3}$), M the molecular mass of Al_2O_3, z the number of electrons used in the anodizing process, and F the faradaic constant, the values obtained also being presented in Table 1. Figure 3 shows the dependence of the increase in thickness on passivation potential for the borate buffer solution pH 7.8. A linear dependence is observed, whose slope yields a ratio of increase of oxide film thickness of $3.6\,nm\,V^{-1}$. The maximum oxide thickness for the potential range examined does not exceed a value of 10.3 nm.

Figures 4 and 5 show that the film growth kinetics involve a linear relation in the $\log i - \log t$ diagram, which can be described by

$$i = kt^{-m} \qquad (3)$$

where i and t denote current and time, and k and m are constants. A linear part, as well as a deviation from linearity, and from Equation 3, is noted at all passivation potentials (Fig. 4). With lower passivation potentials the deviation from linearity is greater and starts sooner (e.g., at a passivation potential of 0.0 V the deviation occurs after 350 s, while the linear current–time dependence is maintained for more than 1000 s at a passivation of 1.2 V). Figure 5 shows current–time responses for passivation at a potential of 0.6 V in borate buffer solutions of different pH. At this potential, a linear $\log i - \log t$ relationship holds for more than 1000 s at pH 6.8. When the pH increases, the deviation from linearity starts sooner. Thus, in a borate buffer solution of pH 9.25, the deviation from linearity of the $\log i - \log t$ plot occurs after 90 s of anodization. The constants from Equation 3, k and m, were determined from the linear part of the $\log i - \log t$ plot. The exponent m represents the slope, while the constant k was determined by extrapolation of the linear part to its intersection with the ordinate for $\log t = 0$ s. Table 1 presents values for k and m for all solutions and potentials. The results indicate that k depends on pH. For passivation of 0.6 V the

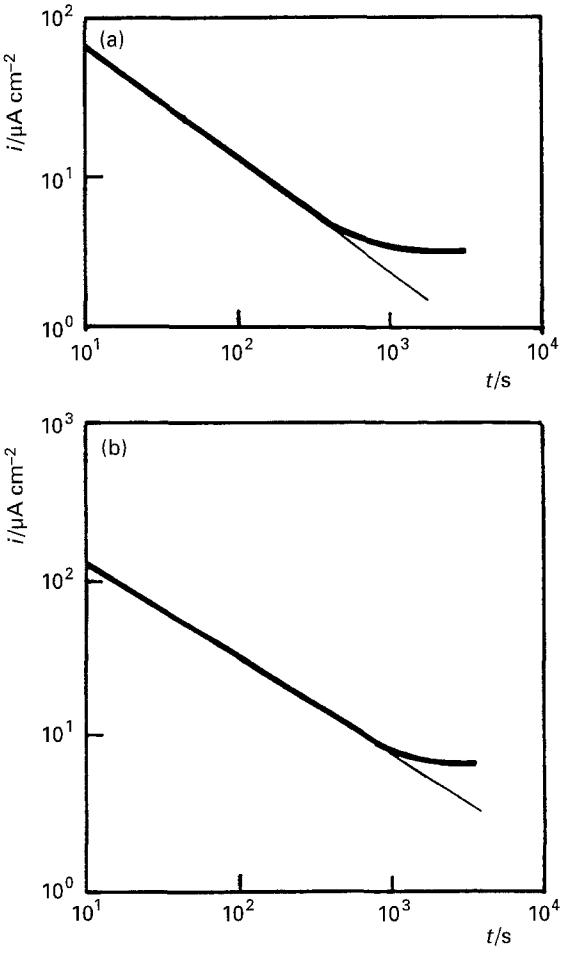

Fig. 4. Decay of anodic current with time in pH 7.8 borate buffer solution after stepping the potential to various values in the passive region (a) 0.0 V; (b) 1.2 V.

values obtained at pH from 6.8 to 8.4 ranged from 0.3 to $0.4\,mA\,cm^{-2}$. The magnitude of m does not depend on pH. The value of 0.64 was obtained for all solutions examined. The effect of the potential on the oxide film growth kinetics was analysed in detail in the solution of pH 7.8; when the passivation potential increases from −0.2 to 2.0 V the value of the constant k increases from 0.3 to $0.8\,mA\,cm^{-2}$, while the constant m decreases from 0.73 to 0.59.

The results indicated in Figs 4 and 5 show that after a short time (about 20 s) the anodic current slowly and continuously decreases with time. Eventually a steady-state is reached. At this stage the $\log i - \log t$ plot deviates from linearity. The steady-state current is generally related to the rate of electrochemical dissolution of metal through the passive film and chemical dissolution of the oxide, so that it is a measure of the protective capabilities of the oxide. The steady-state current is potential and pH dependent. Figure 6 shows the change in this current with potential for a borate buffer solution of pH 7.8. A linear dependence of $\ln i_{ss}$ on the potential applied is observed. Figure 7 indicates the dependence of the current on pH. A marked growth in the steady-state current is noticed, and the values for i_{ss} are up to ten times higher in alkaline solutions (pH 9.25) than in neutral ones.

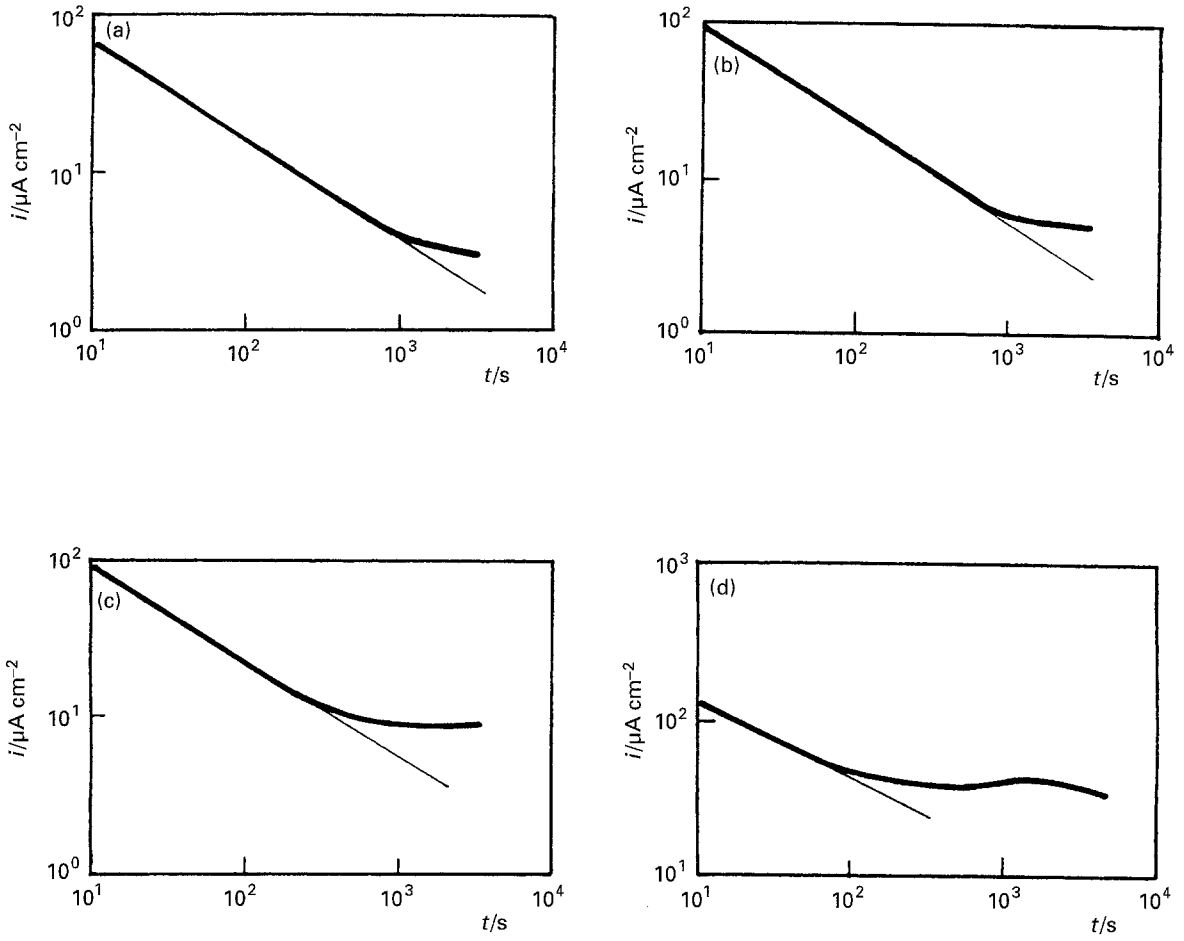

Fig. 5. Decay of anodic current with time at 0.6 V in (a) pH 6.8; (b) pH 7.8; (c) pH 8.4; (d) pH 9.25 borate buffer solutions.

3.3. *Impedance measurements*

Figure 8 represents complex plane impedance plots for different electrode potentials in a borate buffer solution of pH 7.8. For all potentials, the response of the system in the Nyquist complex plane (Fig. 8(a)) was a semicircle whose diameter increased with increase in potential. A more convenient method, which better shows the frequency dependence of the impedance data is the so-called Bode diagram (Fig. 8(b)). The high frequency limit ($f > 1$ kHz) corresponds to the electrolyte resistance, R_{el}. The low frequency limit ($f < 1$ Hz) represents the sum of R_{el} and the resistance R_1, which is, in the first approximation, determined by both the electronic conductivity of the oxide film and the polarization resistance of the dissolution and repassivation processes. In these two borderline cases (at high and at low frequency) the phase angle between current and potential, θ, assumes a value of $\sim 0°$, corresponding to the resistive behaviour of R_{el} and $(R_{el} + R_1)$. At medium frequencies capacitive behaviour of the system is evident, determined by the dielectric properties of the oxide film. The phase shift between current and voltage approaches a value of $\sim 90°$. The capacitive time constant is attributed to the formation of the oxide layer or to the oxide layer itself. Namely, the oxide film is considered to be a parallel circuit of a resistor due to ionic conduction in the oxide, and a

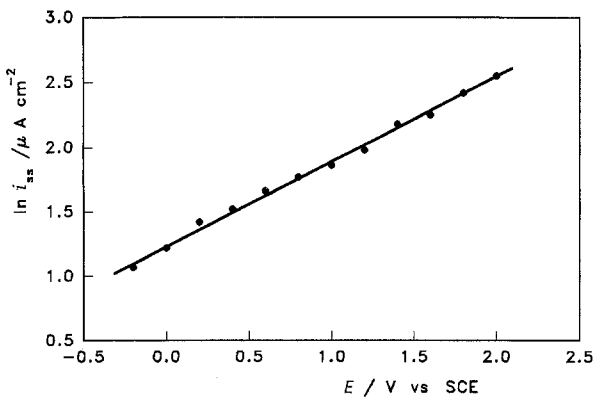

Fig. 6. Steady current relative to the passivation potential for aluminium in the borate buffer solution pH 7.8.

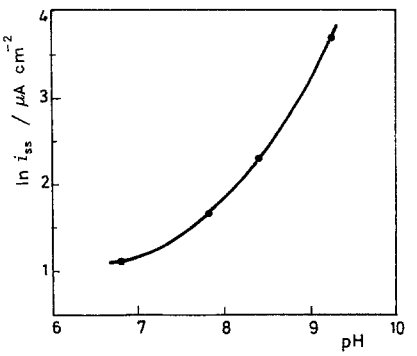

Fig. 7. Steady current relative to the solution pH for passivation at 0.6 V.

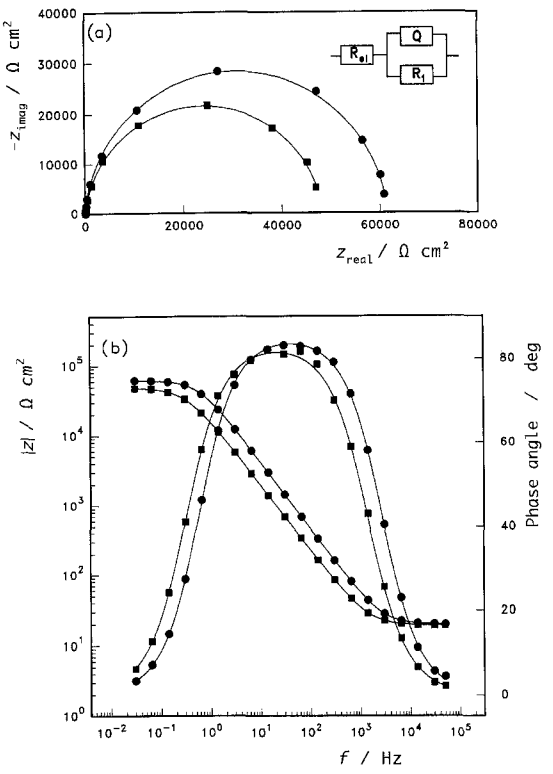

Fig. 8. Impedance diagrams for aluminium in the borate buffer solution pH 7.8 at different potentials in the passive region (■) $E = 0.0$ V and (●) $E = 1.2$ V for (a) Nyquist plot and (b) Bode plot.

capacitance due to the dielectric properties of the oxide.

A mathematical analysis of the impedance diagrams has shown that the centre of the capacitive loop lies somewhat below the real axis, and that the slopes of the $\log|Z|$ against $\log f$ plots are not -1. To describe this response of the passive electrode, a constant phase element, CPE, can be used whose impedance, Z_{CPE}, is described by the expression [17, 18]:

$$Z_{CPE} = [Q(j\omega)^n]^{-1} \quad (4)$$

where Q is a constant. The parameter n is also a constant that can assume different values in the range from -1 to $+1$. According to the magnitude of the value n, the Equation 4 can describe inductivity ($n = -1$), resistance ($n = 0$), Warburg impedance ($n = 0.5$) and capacity ($n = 1$). For the examined system Al/barrier film/electrolyte the calculated values for the parameter n amount to 0.94 ± 0.01 for all potentials and pH values, so that the constant phase element can be substituted by capacity in the proposed equivalent circuit (the detail of Fig. 8(a)). For each set of experimental impedance data the parameters of the equivalent circuit R_{el}, R_1 and CPE ($n = 1$, $Q = C$) were evaluated using a simple least square fit procedure; these values are shown in Table 2. Owing to the depression observed, that is, rotation of the capacitive semicircle under the real axis and the calculated values of the parameter n, the oxide film formed on aluminium cannot be considered to have ideal dielectric properties. In the frequency range from 5 to 500 Hz a phase shift between current and voltage is observed, different from 90°, assuming values from 82° to 86° (depending on the passivation potential). This behaviour has not been completely explained physically, but the explanation may be related to nonhomogeneity within the oxide film mass [19] and the fact that the electrode surface, seen at the microscopic level, is not ideally smooth but has a large number of surface defects, such as projections, cavities, local nonhomogeneities of charge etc. [20].

The data shown in Table 2 indicate that the

Table 2. Results of the analysis of impedance spectras for aluminium as a function of applied potential and solution pH

pH	*E vs SCE* /V	R_{el} /Ω cm²	$Q \times 10^6$ /Ω^{-1} s^n cm^{-2}	*n*	R_1 /kΩ cm²	R_2 /kΩ cm²	*L* /kH cm²	*d* /nm
6.8	0.0	21.69	11.04	0.93	70.28	–	–	0.80
	0.6	22.27	6.90	0.93	89.71	–	–	1.28
	1.2	22.10	4.97	0.94	95.40	–	–	1.78
7.8	−0.2	20.10	14.25	0.93	45.51	–	–	0.62
	0.0	19.18	11.14	0.93	48.30	–	–	0.79
	0.2	19.20	9.31	0.94	50.31	–	–	0.95
	0.4	18.91	8.33	0.93	53.30	–	–	1.06
	0.6	19.10	6.87	0.94	54.50	–	–	1.29
	0.8	20.01	6.75	0.94	57.39	–	–	1.31
	1.0	20.10	5.35	0.95	60.42	–	–	1.65
	1.2	19.91	4.86	0.95	61.50	–	–	1.82
	1.4	19.22	4.56	0.95	63.11	–	–	1.94
	1.6	19.02	4.10	0.94	66.50	–	–	2.16
	1.8	20.21	3.76	0.95	68.57	–	–	2.35
	2.0	18.70	3.53	0.95	70.50	–	–	2.51
8.4	0.0	19.05	10.49	0.95	20.65	–	–	0.84
	0.6	19.01	6.99	0.95	25.53	–	–	1.27
	1.2	18.90	4.94	0.93	31.34	–	–	1.79
9.25	0.0	18.70	20.10	0.93	2.93	1.92	1.31	0.44
	0.6	17.88	6.96	0.94	4.93	3.39	1.73	1.27
	1.2	17.11	3.99	0.95	6.48	4.06	2.19	2.22

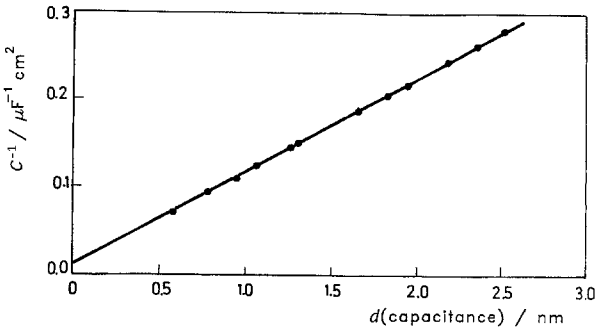

Fig. 9. Reciprocals of capacity relative to the calculated values for the barrier film thickness for aluminium in the borate buffer solution pH 7.8.

resistance of the oxide film increases linearly with increase in the passivation potential, so that this value increases by 20 kΩ cm^2 for an increase of 2.0 V in the passivation potential. Furthermore, it can be seen in Table 2 that the measured capacity decreases from 14.25 to 3.53 μF cm^{-2} with increase in the passivation potential from −0.2 to 2.0 V. As a first approximation the capacitance may be related to a series connection between the double layer capacity (C_{dl}) and the oxide layer capacity (C_{ox}) according to the usual expression:

$$1/C = 1/C_{dl} + 1/C_{ox} \quad (5)$$

where

$$C_{ox} = \varepsilon\varepsilon_0/d \quad (6)$$

with ε_0 the permittivity of the free space ($\varepsilon_0 = 8.85 \times 10^{-12}$ F m^{-1}), and ε the dielectric constant of the oxide. Since C_{ox} diminishes with increasing oxide film thickness, the total capacity C should decrease with increasing electrode potential in agreement with the results given in Table 2. Taking $\varepsilon = 10$ for Al_2O_3 [21], the thickness of the barrier films was calculated. In calculation of the barrier film thickness, C_{dl} was assumed to be much higher than C_{ox}, and its effect on the overall impedance was assumed to be negligible. The validity of this assumption was confirmed by the results of Fig. 9 where the reciprocals of the capacity measured and the calculated values for oxide thickness are plotted. Extrapolation of the straight line, to its intersection with the ordinate determined the actual value of the double layer capacity which amounted to 77 μF cm^{-2} for the borate buffer solution pH 7.8. Figure 10 shows the dependence of the barrier film thickness on the passivation potential. A linear dependency can be observed, whose slope yielded a ratio of increase of oxide film thickness of 0.85 nm V^{-1}. The maximum thickness of the barrier film in the potential range examined does not exceed 3 nm.

It should be pointed out that the thickness of barrier films on aluminium, as determined by impedance measurements (i.e., determination of capacity) is several times smaller than that estimated from the measured quantity of charge used during the anodizing process. This is probably due to the fact that anodic processes contributing to the current can include other processes beside formation of the oxide film: dissolution of metal through the oxide film, as well as chemical dissolution of the oxide, and evolution of oxygen. Each of these processes may take place in parallel with formation of the barrier film on the aluminium surface. To estimate the charge used for subordinate dissolution reactions, it is necessary to determine current efficiency. The relation between the oxide film thickness as determined by capacity measurements and that determined by the quantity of charge used per unit surface during the anodizing process, yields a straight line (Fig. 11) whose slope can be used to determine current efficiency [19]. Current efficiency determined in this way amounts to 22% and indicates that only a small part of the overall anodic current measured is used in the formation of the oxide film. Similar values were obtained for other solutions. The current efficiency for oxide growth is 21, 19 and 21% for solutions of pH 6.8, 8.4 and 9.25, respectively. The formation of the barrier film is obviously a process that takes place with large current losses.

Figure 12 shows the effect of the solution pH on system responses in impedance measurements, for the case when passivation was carried out at a potential of 0.6 V. An increase in pH up to 8.4 is observed to cause a decrease in the overall impedance of the system, while the shape of the impedance diagram remains the same. Marked changes are again observed

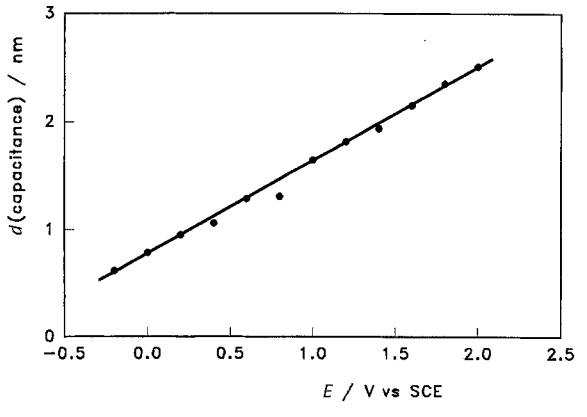

Fig. 10. Barrier film thickness (determined from capacity) relative to passivation potential for aluminium in the borate buffer solution pH 7.8.

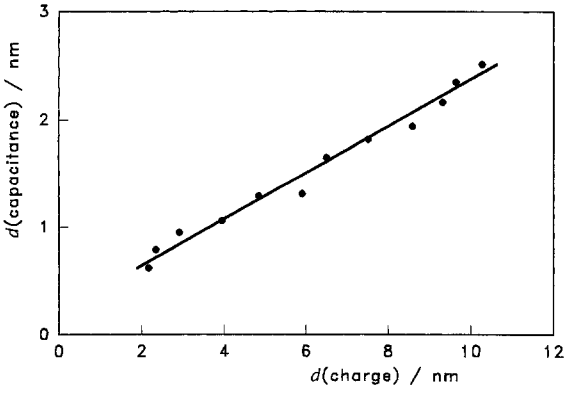

Fig. 11. The thickness of the barrier film formed on aluminium in the borate buffer pH 7.8 solution calculated from the capacitance and the anodic charge passed. The slope of the solid line represents the efficiency of film formation.

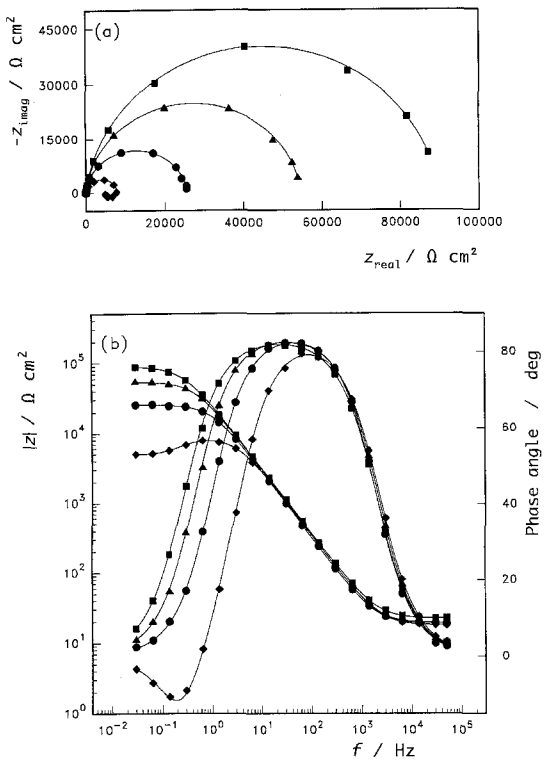

Fig. 12. Impedance diagrams for aluminium at a passivation at 0.6 V in borate buffer solutions with (■) pH 6.8; (▲) pH 7.8; (●) pH 8.4; (◆) pH 9.25 for (a) Nyquist plot and (b) Bode plot.

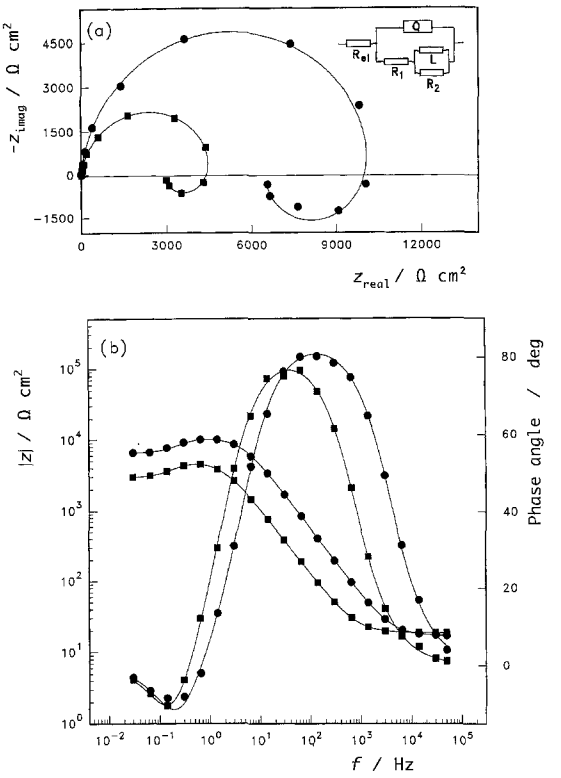

Fig. 13. Impedance diagrams for aluminium in the borate buffer solution pH 9.25 at different potentials in the passive region (■) $E = 0.0$ V and (●) $E = 1.2$ V for (a) Nyquist plot and (b) Bode plot.

in the solution of pH 9.25. In passivation carried out in this borate buffer solution, the response in the complex impedance plane for all the potentials examined (Fig. 13) deviates from the usual capacitive behaviour, and an inductive loop is observed at low frequencies ($f < 1$ Hz). The existence of the inductive loop is still not explained and neither is its dependence on the potential. The inductive loop is probably due to the relaxation processes in adsorbed species formed during dissolving at the oxide/electrolyte interface which define the faradaic processes. An equivalent circuit, shown in the detail of Fig. 13(a) has been proposed for this response in the complex impedance plane. The equivalent circuit consists of a CPE (substituting for capacity in the equivalent circuit $n = 1$, $Q = C$) in parallel to series resistors R_1 and R_2 and an inductance L in parallel to R_2. Table 2 presents their values relative to potential. The impedance corresponding to the equivalent circuit consisting of R_1, R_2, C and L may be considered as a general term, including faradaic impedance effects. The characteristic values of Z_f are the charge transfer resistance, R_{ct}, and the polarization resistance, R_p. The charge transfer resistance corresponds to the sum of R_1 and R_2 and the polarization resistance to R_1. The data in Table 2 indicate that the values of R_1 decrease by an order of magnitude when the solution pH increases in passivation at a constant potential. However, it is surprising that this direction of change is not accompanied by a corresponding reduction in the oxide film thickness. According to data in Table 2, the thickness of the oxide film does not depend on the solution pH. The value of 1.28 ± 0.01 nm was obtained for all the solutions for passivation at 0.6 V, which could be considered constant. The answer to the question why the film formed in a solution of a higher pH provides a lower resistance to current does not lie only in the reduction of the barrier film thickness. The reduction of resistance can be brought about by changes in its structure as well as composition, which is supported by the current–time responses obtained.

The results can be understood in terms of two point defect models for passive film growth [6–11]. The point defect model proposed by Macdonald *et al.* [9–11] is the more quantitative of the two. In this model, the film growth is due to a flux of cation vacancies from the film/solution interface to the metal/film interface and to a flux of oxygen vacancies in the opposite direction. Both interfaces are assumed to be under electrochemical equilibrium. Additional assumptions in this model include the electrical potential across the film/solution interface being a linear function of the applied voltage and the pH of the solution, and the electric field strength being constant within the film. In agreement with the theory proposed the authors of the model have derived equations for the steady state current and the barrier film thickness. These equations can be compared directly with the experimental data and predict that the stationary thickness and the logarithm of the steady state current will vary linearly with change of the passivation potential. Based on these linear relations, empirical parameters can be determined which reflect the dependence of the potential drop at the phase interface oxide/electrolyte on the potential applied and on the solution pH.

The results confirm a linear dependence of $\ln i_{ss}$ on

the applied voltage, as predicted by this point defect model. The proportionality factor (α) between the potential drop across the film/solution interface and the applied voltage can be calculated from the slope of Fig. 6, and the calculated value of α is 0.006. This small value indicates that only a small portion of the applied voltage drop occurs across the passive film/solution interface. Most of the voltage drop occurs across the film. This can be understood from the data by impedance measurements, which indicate that the value of the polarization resistance is very high due to the presence of the oxide film.

The most important assumption made by the authors in the development of the point defect model was that the electric field within the oxide was constant and did not depend on the potential applied or the oxide film thickness. The constant magnitude of an electric field can be maintained only if the thickness of the barrier film increases linearly with the passivation potential applied. The results shown in Fig. 10 are in accordance with the predictions of this theory and indicate a linear dependence of the barrier film thickness on the passivation potential. The field strength across the oxide is constant and amounts to $1.2 \times 10^7\,\mathrm{V\,cm^{-1}}$.

According to MacDougall's model, the oxide film reaches steady thickness rapidly, and the oxide obtained is extremely defective. Therefore the decay of anodic current with time, in anodic passivation at a constant potential, has been associated with a decrease in the active defect area in the film and not with increased thickness. The rate of increased 'perfection' decreases logarithmically with time and eventually the steady state is reached. At this stage no further improvement of the film takes place. Anodic charge consumption is mainly due to localized breakdown and repair of the passive film at defect sites. Most of the charge is associated with metal dissolution during inefficient repair. The solution aggressiveness and the anode potential determine the upper limit of film stability and therefore the extent of linearity between $\log i - \log t$.

Although the current efficiency is only 20%, a linear dependence has been observed between $\log i - \log t$. With less aggressive solutions (lower pH) and higher anodic potentials, the deviation from the $\log i - \log t$ behaviour is encountered later, which is in agreement with the theory outlined. Impedance measurements have confirmed the formation of a barrier film of a better ordered structure in this case. The resistance of the oxide film, expressed by the measured value R_1, can be an indication of orderliness of the structure of the barrier film. In passivation at a constant potential (e.g., 0.6 V) this parameter decreases significantly (from 89.71 to $4.39\,\mathrm{k\Omega\,cm^2}$) with increase in pH (from 6.8 to 9.25), although the barrier film thickness does not change (1.28 ± 0.01 nm), while the linear part of the $\log i - \log t$ diagram is shorter. These results are in complete agreement with the MacDougall theory claiming that the oxide reaches steady thickness very rapidly in passivation, and that the decay of the anodic current with time is related to the reduction of defective surfaces in the oxide, and not to the increase of the oxide thickness. If passivation potential increases, barrier films of higher protective capabilities (higher resistance) are formed on aluminium. However, the thickness of the barrier film increases with the increase in potential. In this case the increase in resistance may be due to the increased thickness, and not to the ordering of the barrier film structure. To establish whether the results obtained fully satisfy the assumptions of the MacDougall theory, additional measurements should be taken which would provide data on the change in oxide thickness, that is, on the resistance relative to duration of anodizing.

4. Conclusion

(i) It has been shown that the a.c. impedance can be applied in analysis of the passive electrode on aluminium, especially as it makes it possible to distinguish the elementary processes taking place at the anode, and to determine the actual thickness of the barrier film.

(ii) The thickness of the barrier film increases linearly with increasing passivation potential (the increment ratio is $0.85\,\mathrm{nm\,V^{-1}}$), while the maximum thickness in the potential interval examined does not exceed 3 nm and can be said to be independent of solution pH.

(iii) The oxide film resistance increases linearly with increasing passivation potential, and decreases markedly with increasing pH (from 6.8 to 9.25), thereby suggesting that a barrier film of lower protective capabilities is being formed.

(iv) Current efficiency in oxide film formation on aluminium is low. The value of ~20% was obtained for all solutions examined.

(v) The growth kinetics of the oxide layer on aluminium fit the defect model proposed by Macdonald *et al.*

References

[1] N. Cabrera and N. F. Mott, *Rep. Prog. Phys.* **12** (1948) 163.
[2] N. Sato and M. Cohen, *J. Electrochem. Soc.* **111** (1964) 512; *ibid.* **111** (1964) 519.
[3] S. Asakura and K. Nobe, *ibid.* **118** (1971) 536.
[4] N. Sato and K. Kudo, *Electrochim. Acta* **19** (1974) 461.
[5] J. L. Ord, J. C. Clayton and D. J. DeSmet, *J. Electrochem. Soc.* **124** (1977) 1714.
[6] B. MacDougall, *ibid.* **127** (1980) 789.
[7] *Idem, ibid.* **130** (1983) 114.
[8] B. MacDougall, D. F. Mitchell and M. J. Graham, *ibid.* **132** (1985) 2895.
[9] C. Y. Chao, L. F. Lin and D. D. Macdonald, *ibid.* **128** (1981) 1187.
[10] L. F. Lin, C. Y. Chao and D. D. Macdonald, *ibid.* **128** (1981) 1194.
[11] D. D. Macdonald and M. Urquidi-Macdonald, *ibid.* **137** (1990) 2395.
[12] C. G. Wood, 'Porous anodic films on aluminium', *in* 'Oxide and Oxide Films', vol. 2 (edited by J. W. Digle and K. Vijh), Marcel Dekker, New York (1972).
[13] A. Despić and V. P. Parkhutik, 'Electrochemistry of aluminium in aqueous solutions and physics of its anodic oxide',

in 'Modern Aspects of Electrochemistry', vol. 20 (edited by J. O'M. Bockris, R. E. White and B. E. S. Conway), Plenum Press, New York (1989).
[14] H. J. de Wit, C. Wijenberg and C. Crevecoeur, *J. Electrochem. Soc.* **126** (1979) 779.
[15] J. B. Bessone, C. Mayer, K. Yüttner and W. J. Lorenz, *Electrochim. Acta* **28** (1983) 171.
[16] J. B. Bessone, D. R. Salinas, C. Mayer, M. Ebert and W. J. Lorenz, *ibid.* **37** (1992) 2283.
[17] J. R. Macdonald and W. B. Johanson, 'Theory', *in* 'Impedance Spectroscopy', (edited by J. R. Macdonald), J. Wiley & Sons, New York (1987).
[18] Z. Stoynov, *Electrochim. Acta* **35** (1990) 1493.
[19] J. A. Bardwell and M. C. H. McKubre, *ibid.* **36** (1991) 647.
[20] U. Rammelt and G. Reinhard, *ibid.* **35** (1990) 1045.
[21] J. Hitzig, K. Yüttner, W. J. Lorenz and W. Paatsch, *Corros. Sci.* **24** (1984) 945.